ACS OMEGA

http://pubs.acs.org/journal/acsodf

Article

Accurate and Model-Free Control Function for a Single Stage Transcritical Refrigerator Cycle

Johan González, Fèlix Llovell, José Matías Garrido,* and Héctor Quinteros-Lama*

Cite This: *ACS Omega* 2020, 5, 19217−19226

Read Online

ACCESS | Metrics & More | Article Recommendations

ABSTRACT: Transcritical cycles are a successful and probed system in engineering practices, particularly in refrigeration. Therefore, their optimization is a critical factor in the design, control, and operation in order to maximize the coefficient of performance (COP) and to find the optimal pressure operating conditions. Often, this labor is faced using empirically based correlations, which are limited by their origin and the configuration of the cycle. In this regard, this work is devoted to the development of a rigorous and general framework in order to characterize the behavior and performance of a simple transcritical refrigeration cycle. An accurate mathematical expression for the COP depending on the compressor efficiency and the properties of the working fluid is presented. The expression proposed has no approximations and is relevant to any model depending on the Helmholtz variable group, being easy to combine with any equation of state (EOS), regardless of its complexity. From this expression, it is possible to derive a simple control function for transcritical refrigeration cycles. As an example, the expression is combined with the Span−Wagner EOS, presenting a comprehensive application for a transcritical cycle using CO_2 and N_2O as working fluids.

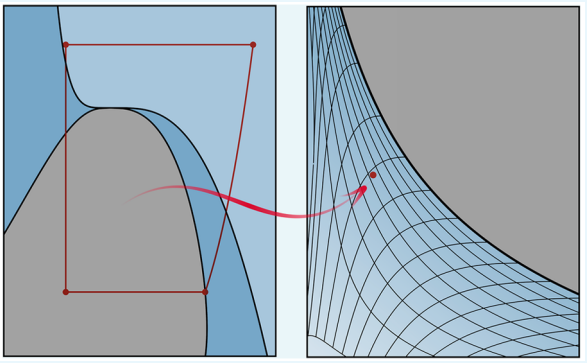

1. INTRODUCTION

The high-energy demand in the world has become a focus of attention for researchers in the last decades because of the constant quest to look for alternative processes able to produce power with a low economical and environmental cost. Notably, in the refrigeration and heat pump industry, working fluids with zero ozone depletion potential (ODP) and a lower global warming potential (GWP) are required. From an environmental viewpoint, the Montreal Protocol[1] phased-out chlorofluorocarbons (CFCs) and hydrochlorofluorocarbons (HCFCs) because of their high ODP. They were progressively substituted by ozone-friendly hydrofluorocarbons (HFCs), which had been considered as permanent replacement fluids and widely used in refrigeration processes.[2] However, they have been lately classified on the list of regulated substances because of their high GWPs, and the recent Kigali Amendment to Montreal Protocol,[3] along with European and other international regulations, has established further restrictions limiting the use of these compounds. In this situation, alternative fluids, such as CO_2, have received much attention because of their null ODP, low GWP, non-toxicity, non-flammability, and adequate thermodynamic properties[4−8] compared to other synthetic refrigerants.[9,10] Remarkably, CO_2 has a critical temperature near ambient temperature (T_c = 304.128 K[11]), a reasonably low critical pressure (P_c = 7.3773 MPa[11]), and a critical density (ρ_c = 467.6 kg/m^3[11]) higher than most other supercritical solvents.

Considering the fact that the critical temperature of CO_2 is lower than the typical values of the heat rejection temperature of air-conditioning, refrigeration systems using CO_2 are capable of performing their process on different thermodynamic states, in which the heat rejection process takes place above the supercritical pressure, while the evaporation process occurs at subcritical conditions. Thus, the analysis of the so-called transcritical cycle presents a challenge, not only from a theoretical perspective but also from a practical interest. In this respect, enhancement in the performance of the CO_2 transcritical cycle has been achieved from the modification of basic cycles, replacement and addition of fluid components in the system, and optimization of critical variables.

From a theoretical perspective, apart from having a good equation of state (EOS) to adequately assess the appropriate performance of cycles in terms of thermodynamic properties, it

Received: June 7, 2020
Accepted: July 3, 2020
Published: July 20, 2020

is still necessary to establish which are the optimal ranges on the operational variables (i.e., temperature, pressure, and isentropic efficiency) and how they are interrelated. Moreover, the accurate prediction of thermo-mechanical ranges where these behaviors may occur is still an open problem to design appropriate operating conditions.

Thus, from an operational viewpoint, optimization of the discharge pressure in the CO_2 cycle has been done for air conditioning applications, and various methods have been proposed. Among these studies, it is important to highlight the contributions of Inokuty,[12,13] who developed a witty graphical approach to obtain the optimum compression ratio of a transcritical cycle using literature data. Later, Kauf[14] was the first to propose a control function, which is a simple empirical function to relate the ambient temperature with the optimal operating pressure of the transcritical cycle. The aforementioned approach has the advantage that it allows us to easily obtain a result in contrast with the time-consuming graphical methodology. Following the work of Kauf, other works expanded the idea of a control function to other variables of the transcritical cycle. One of the most commonly applied control functions is the correlation developed by Liao et al.,[15] which considers not only the cooler or ambient temperature but also the evaporator temperature. Other empirical control functions have been developed from different approaches considering different variables,[14−23] based on the same premises of the control function first developed by Kauf.[14] A complete review of control functions is presented by Yang et al.[24]

Furthermore, Yang et al.[24] compared different optimal high-pressure correlations of transcritical CO_2 in the calculation of the coefficient of performance (COP). They found that adjusting the optimal discharge pressure together with the isentropic efficiency of the compressor using off−line correlations[17−23,25−28] results in the prediction of false COP values. At the same time, the comparison with the real-time high-pressure optimization methods[29−33] provides a more efficient and robust solution. Of course, although the second method is more effective than the first one, the necessity of real operational data is much more complex and less cost-effective. Otherwise, control functions are empirically based mathematical expressions able to characterize the optimal operating conditions of a cycle. These kinds of functions are widely used for different purposes,[34] and similar approaches may be developed for other configurations of cycles, other working fluids,[35] or even mixtures of working fluids.[36,37] The inherent empirical nature of these functions give then the advantage of simplicity, but their weaknesses are also significant. First, the most obvious issue is that control functions are substance-specific; therefore, different models of arbitrary fluids cannot be coupled. Additionally, they are limited to narrow ranges[24] and often include a limited number of variables. Indeed, most control functions model the optimal conditions at different variables, and hence, the behavior of the COP around the extreme value is unknown.

The main objective of this work is to present a rigorous and general framework able to describe the optimal operating conditions of a transcritical cycle. This development constitutes an analytical and non-explicit control function, which allows any internal model to obtain numerical results. The advantages of this framework, in contrast to traditional control function approaches,[24] are significant. First, the mathematical structure is a model-free approach depending on the Helmholtz energy function. Hence, it may be coupled with an equation of state using an arbitrary working fluid, removing the limitations of the compound-specific control function, which often are only available for carbon dioxide. Moreover, non-idealities and assumptions such as isentropic compression or the isobaric cooling process can be easily included. In addition, all the variables of the transcritical cycle can be taken into account, and even the same framework can be adapted to the optimization of the process through experimental data. Finally, considering different assumptions and simplifications, any control function can be obtained directly from this framework. In order to demonstrate the capabilities of the present approach, the CO_2 is selected as the working fluid, and the Span−Wagner EOS,[4] a highly accurate model for CO_2, is used as the internal model. As a result, a theoretically based control function capable of relating the variables of a single-stage transcritical refrigeration cycle is presented.

2. RESULTS AND DISCUSSION

2.1. Analytical Optimum in a Simple Transcritical Cycle. The COP of a refrigeration cycle is given by the ratio between the extracted heat in the evaporation unit and the amount of work inverted in the compression stage.[38] In addition, it is known that there is an optimum value of the COP depending on the ratio of compression[24,39−42] in a simple transcritical cycle. Then, considering a single-stage transcritical cycle with an efficiency, η, for the adiabatic compressor unit, and using the terminology shown in Figure 1 for each stage of the cycle, the COP of the process is given by

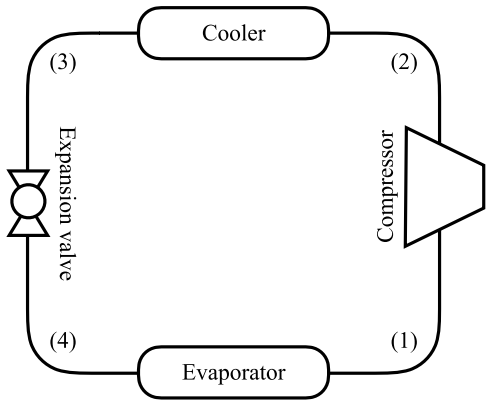

Figure 1. Schematic representation of a simple transcritical refrigeration cycle composed by an evaporator, gas compressor, gas cooler, and an expansion valve.

$$\mathrm{COP} = \frac{Q}{W} = \frac{\tilde{H}_1 - \tilde{H}_4}{\tilde{H}_2 - \tilde{H}_1} = \eta \frac{\tilde{H}_1 - \tilde{H}_4}{\tilde{H}_2^{\mathrm{r}} - \tilde{H}_1} \quad (1)$$

where $\tilde{H}_i$ is the molar enthalpy at point i, and the superscript r concerns with the reversible approximation of the outlet of the adiabatic compressor unit. Moreover, $\tilde{H}_3 = \tilde{H}_4$. Consequently, eq 1 yields

$$\mathrm{COP} = \eta \frac{\tilde{H}_1 - \tilde{H}_3}{\tilde{H}_2^{\mathrm{r}} - \tilde{H}_1} \quad (2)$$

The slope of the COP as a function of the outlet pressure of the compressor, P_2, is given by

https://dx.doi.org/10.1021/acsomega.0c02681
ACS Omega 2020, 5, 19217−19226

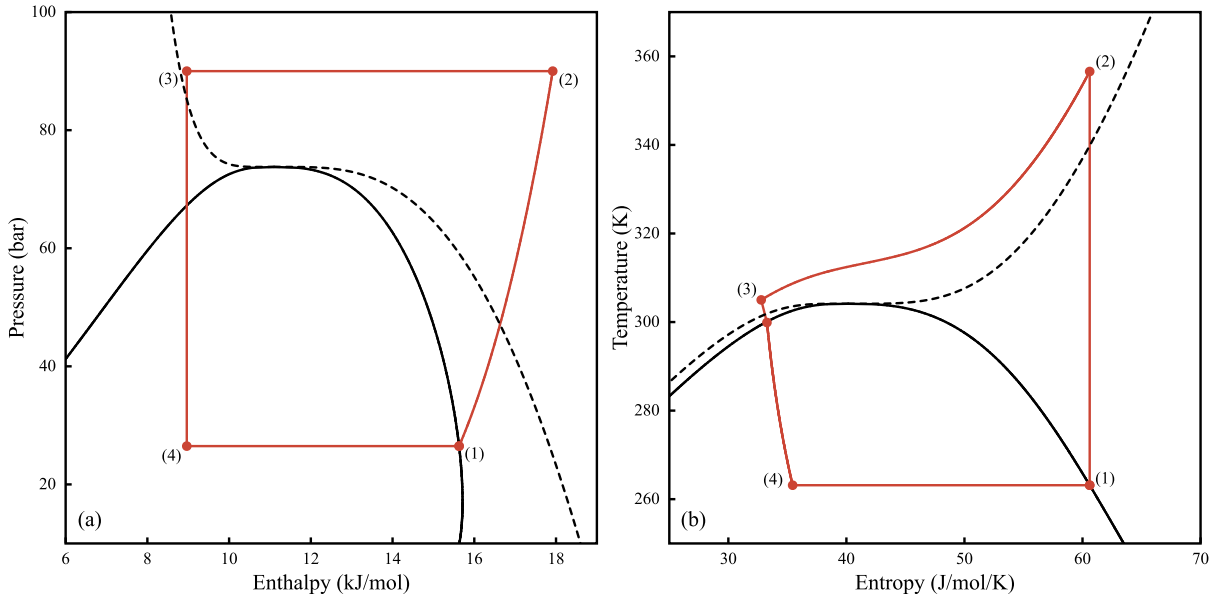

Figure 2. (a) Pressure vs enthalpy and (b) temperature vs entropy diagrams as predicted by the Span−Wagner EOS for CO_2. A representation of a simple transcritical cycle is displayed in crimson lines. The numbers correspond to (1): outlet of the evaporation stage, (2): outlet of the compressor unit after an isentropic process, (3): outlet of the cooling unit, and (4): outlet of the expansion valve.

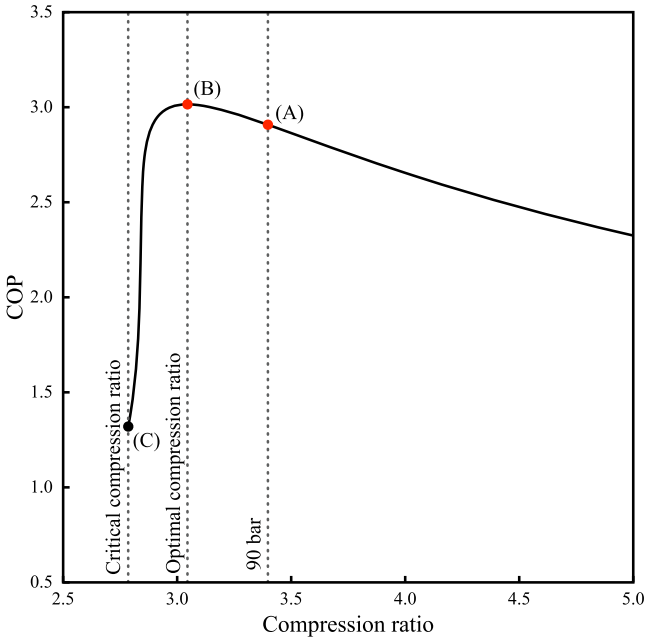

Figure 3. Behavior of COP as a function of the compression ratio, r, as predicted by the Span−Wagner EOS, using fixed temperatures in the outlet of the evaporator and cooling unit of T_1 = 263.15 K and T_3 = 305.00 K, respectively.

$$\frac{\mathrm{dCOP}}{\mathrm{d}P_2} = -\frac{1}{\tilde{H}_2^{\mathrm{r}} - \tilde{H}_1}\left(\left(\frac{\mathrm{d}\tilde{H}_2^{\mathrm{r}}}{\mathrm{d}P_2}\right)_S \mathrm{COP} + \eta\left(\frac{\mathrm{d}\tilde{H}_3}{\mathrm{d}P_2}\right)_T - (\tilde{H}_1 - \cdots \cdots \tilde{H}_3)\frac{\partial\eta}{\partial P_2}\right) \quad (3)$$

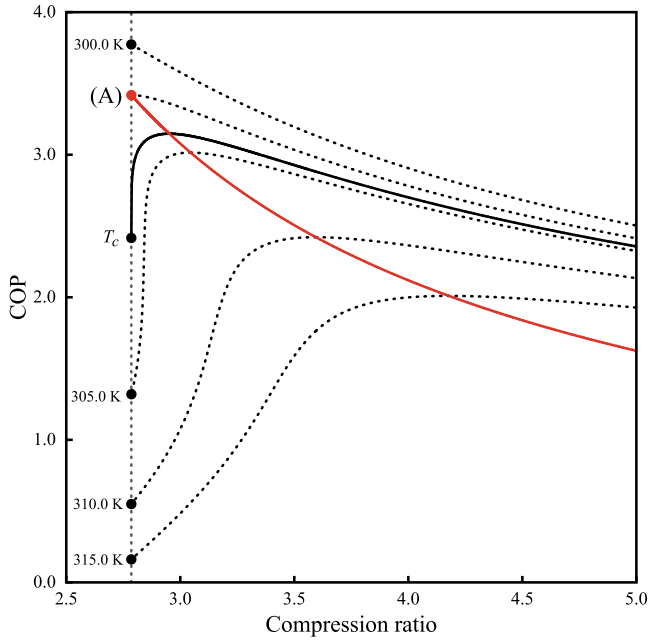

Figure 4. Behavior of COP as a function of the compression ratio, r, at different cooler temperatures (300.00, 302.55, 304.13, 305.00, 310.00, and 315.00 K) as predicted by Span−Wagner EOS, using a fixed temperature at outlet of the evaporator unit of 263.15 K. Point (A) concerns the operational limit for the optimal behavior of the transcritical cycle.

$$\frac{\mathrm{dCOP}}{\mathrm{d}P_2} = -\frac{1}{\tilde{H}_2^{\mathrm{r}} - \tilde{H}_1}\left(\left(\frac{\mathrm{d}\tilde{H}_2^{\mathrm{r}}}{\mathrm{d}P_2}\right)_S \mathrm{COP} + \eta\left(\frac{\mathrm{d}\tilde{H}_3}{\mathrm{d}P_2}\right)_T - (1 - \cdots \cdots \Psi_3)\Delta\tilde{H}_1\frac{\partial\eta}{\partial P_2}\right) \quad (4)$$

where the terms within the parentheses are the changes of the enthalpy as the ratio of compression increases at constant

https://dx.doi.org/10.1021/acsomega.0c02681
ACS Omega 2020, 5, 19217−19226

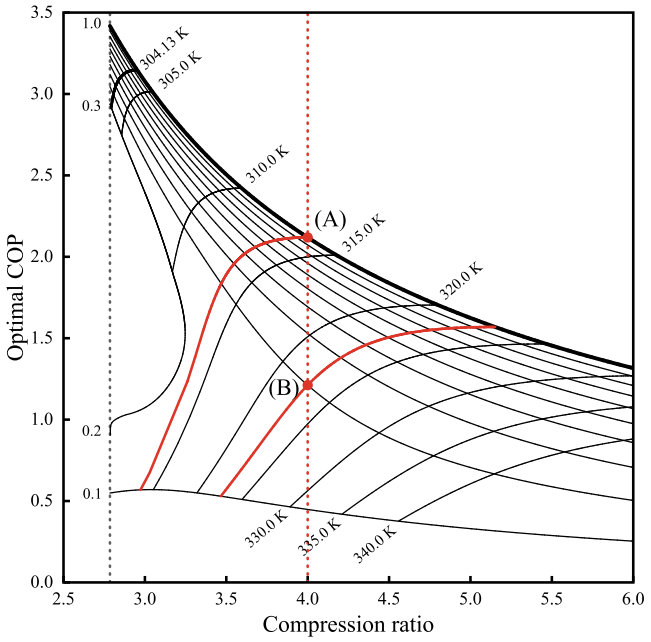

Figure 5. Parametric map of the optimal behavior of the CO_2 transcritical cycle as predicted by Span–Wagner EOS using a fixed temperature in the outlet of the evaporator unit of 263.15 K considering a compression efficiency, η, from 0.1 to 1.0, and temperatures of the cooler from 302.55 to 340.00 K. Points (A) and (B) concern two example optimal systems described in the text.

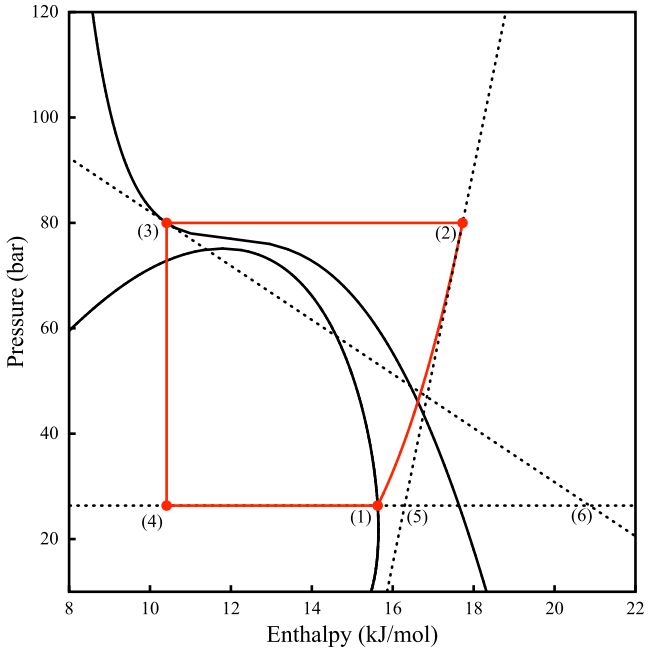

Figure 6. Schematic representation of the graphical approach proposed by Inokuty,[12,13] which can be obtained from the general control function of eq 4.

Table 1. Parameters for the Extension of Kauf's Control Function[14] Considering Different Evaporator Operation Temperatures from 263.15 to 283.15 K

i/j	θ_1	θ_2
1	3.2058	−24.9160
2	-1.3572×10^{-2}	2.9597×10^{-1}

entropy and temperature, respectively. On the one hand, using the fundamental definition of enthalpy, it is easy to obtain that

$$\left(\frac{d\tilde{H}_2^r}{dP}\right)_S = \tilde{v}_2^r \tag{5}$$

On this point, it is essential to keep in mind that $\tilde{v}_2^r$ refers to the volume after an isentropic expansion, and therefore, it will depend not only on configurational contributions but also on thermal contributions. On the other hand, applying the Maxwell relation for enthalpy, we obtain

$$\left(\frac{d\tilde{H}_3}{dP_2}\right)_T = T_3\left(\frac{d\tilde{S}_3}{dP_2}\right)_T + \tilde{v}_3 \tag{6}$$

or, applying systematic Legendre transforms,[43] we obtain

$$\left(\frac{d\tilde{H}_3}{dP_2}\right)_T = \tilde{v}_3 - T_3\frac{\partial^2\tilde{G}_3}{\partial T_3 \partial P_2} \tag{7}$$

because entropy is given by $\tilde{S}_3 = -\partial\tilde{G}_3/\partial T_3$.

Furthermore, the efficiency of the compression unit is often given by an empirical expression as a function of the inlet and outlet compressor pressures. In most convoluted cases, the compressor efficiency may depend on other additional variables, such as the inlet temperature and the mass flow.[44] In these cases, the mathematical labor is equivalent, giving an adequate treatment to the compressor-efficiency function.

Combining eqs 4, 5, and 7, including the vapour fraction in the evaporator unit as $\tilde{H}_1 - \tilde{H}_3 = (1 - \Psi_4)\Delta\tilde{H}_1$, and after some algebra, an analytical expression for the optimal COP is obtained

$$\frac{COP_{op}}{\eta} = \frac{T_3}{\tilde{v}_2^r}\frac{\partial^2\tilde{G}_3}{\partial T_3\partial P_2} - \frac{\tilde{v}_3}{\tilde{v}_2^r} - (1 - \Psi_4)\frac{\Delta\tilde{H}_1}{\tilde{v}_2^r}\frac{\partial \ln \eta}{\partial P_2} \tag{8}$$

where $\Delta\tilde{H}_1$ is the vaporisation enthalpy at pressure P_1 and Ψ_4 is the vapour fraction at point (4). From eq 8, it may be noticed that the optimal compression ratio will not be sensitive to the efficiency of the compressor if the functionality of this value is not abrupt.[15,34,45,46] In an extreme case, if a constant efficiency is assumed, eq 8 is reduced to a more straightforward expression given by

$$\frac{COP_{op}}{\eta} = \frac{T_3}{\tilde{v}_2^r}\frac{\partial^2\tilde{G}_3}{\partial T_3\partial P_2} - \frac{\tilde{v}_3}{\tilde{v}_2^r} \tag{9}$$

The optimal COP value is strongly dependent on the compound, the outlet temperature of the cooler unit and the compression ratio, $r = P_2/P_1$. Finally, the derivative of the Gibbs energy function present in eq 8 can be expressed applying Legendre transforms[43] as

$$\frac{\partial^2\tilde{G}_3}{\partial T_3\partial P_2} = -\frac{\tilde{A}_{vT}}{\tilde{A}_{2v}} \tag{10}$$

where $\tilde{A}$ is the Helmholtz energy function and their subscripts are the partial derivatives using the Rowlinson's shortcut for the derivatives of the thermodynamic functions.[47] It is important to notice that eq 8 is completely analytical for any equation of state, independent of its complexity, because its structure depends on the Helmholtz variable group. Therefore, the model-free nature of this approach allows to be coupled to any model, such as a multiparameter EOS such Span–Wagner,[4,48] tabulated approaches[49] or even a molecularly

https://dx.doi.org/10.1021/acsomega.0c02681
ACS Omega 2020, 5, 19217−19226

Table 2. Parameters for the Theoretically Based Control Function Proposed in This Work Depending on Temperatures, Optimal COP, and Optimal Compression Ratio for Carbon Dioxide and Nitrous Oxide

	carbon dioxide			nitrous oxide		
κ_{ij}	j			j		
i	1	2	3	1	2	3
1	0.14926	−0.25032	−9.40454	−0.01382	−0.00692	5.98685
2	−2.89363	4.83187	−2.30512	0.17673	−0.20977	0.23689
3	2.29127	−3.86783	1.88606	0.10179	−0.22344	−0.04778
4	3081.83433	−5250.34162	2282.25052	2228.71741	−3667.97688	1568.49648
5	128.60168	−258.90105	−39047.20332	56.32352	−117.27132	−23302.10334
6	5558.57914	−11343.49215	9867.05269	2545.98096	−5378.46891	4769.50445
7	83.63715	−251.31456	−7280.75242	82.01015	−211.80192	−3334.50559
8	−5565.44802	11168.94350	−2230.89631	2518.30166	5221.02803	−1171.21570
9	−0.18718	1.41716	−0.20651	−3.58305	8.22818	−3.43543
10	26.39708	−58.03580	34.72192	−3.23926	−8.58106	13.16498
11	−5.62365	24.76083	−23.08220	−21.44896	26.37345	−2.74116
12	19.26477	−49.48211	32.21640	80.32090	−131.68253	48.29887
13	0.00000	0.00000	266731.82951	0.00000	0.00000	23879.43297
14	0.00000	0.00000	0.03521	0.00000	0.00000	0.39540
15	−707.07216	1187.79376	−505.40882	−350.02604	567.83315	−234.25531
16	1489.96126	−2498.79125	1062.76581	750.79726	−1215.21645	501.39850
17	−786.39320	1316.06487	−558.66978	−403.52352	651.08063	−267.83006

Table 3. AAD of the Proposed Control Function Applied to Calculate Different Properties of the Transcritical Cycle of CO_2 and N_2O in the Proposed Range of Evaporator Temperature and Isentropic Efficiency

			AAD	
property	via	eqs	CO_2	N_2O
$\tilde{v}_2^r$	T_3	17	0.07	0.09
$d\tilde{H}_3/dP_2$	T_3	18	0.05	0.02
COP	R	19	0.07	0.08
COP	T_3	17 and 18	0.10	0.00
T_3	COP, r	17−19	0.90	0.03
R	COP.	17−19	0.98	0.11
H	COP, r	17−19	4.61	0.87

based EOS such as SAFT-family EOS,[50−52] or adapting the range of parameterization to the required conditions.

2.2. Analytical Optimisation of a Transcritical Cycle. In order to illustrate the optimization of a transcritical cycle using the mathematical expression presented in Section 2.1, a simple configuration of a CO_2 transcritical cycle is schematically plotted in Figure 1. The cycle is composed by a compressor, a gas cooling unit, a throttling valve, and an evaporator. The stages of the process can be summarized as follows: from (1) to (2), an isentropic compression with an efficiency η is carried out; from (2) to (3), an isobaric cooling process takes place; and from (3) to (4), the fluid crosses the valve through an isenthalpic and adiabatic expansion. Finally, from (4) to (1), an isobaric evaporation process from an equilibrium state to a saturated vapour or, eventually, a superheated vapour occurs.

As a base case, the operating temperature of the evaporator unit is fixed at $T_1 = T_4 = 263.15$ K, which is a usual temperature of a transcritical refrigeration cycle operating with CO_2.[24] Additionally, the compression stage operates isentropically ($\eta = 1.0$) and achieves a pressure of 90 bar, and the cooling unit may lower the temperature of the fluid until the near critical temperature of the compound ($T_3 = 305.00$ K). The phase diagram of the above benchmark is illustrated in Figure 2 in the pressure versus enthalpy projection and in the temperature versus entropy projection.

At the aforementioned conditions and using the Span−Wagner EOS, a COP = 2.750 is found, which corresponds to the performance of the cycle highlighted as (A) in Figure 3. By visual inspection, it is clear that the value of (A) is not the optimum COP value, which is achieved at a lower compression ratio at point (B). This point is directly characterized by eq 8, giving a COP value of 2.777, representing the optimum COP the cycle can reach when the cooling unit works at 305.0 K, and the evaporator unit has fixed properties. Furthermore, the usual behavior of the COP of this kind of cycles as a function of compression ratio is also shown in Figure 3. On the one hand, it is easy to observe that for a compression ratio $P_2/P_1 = r > r_{op}$, the COP decreases systematically because of the increase of the amount of work required by the compressor. On the other hand, a compression ratio lower than the optimum produces a dramatic decrease of the COP until point (C).

At supercritical pressures, the isobaric cooling process is carried out in a homogeneous phase; hence, the gas can be cooled until any temperature. This latter has a technical and operational limit related to the outlet temperature of the cooling unit that can be reached by heat exchange with a readily available media. For this reason, it is interesting to analyze the behavior of the maximum COP and these temperature changes. Figure 4 shows the expected behavior considering the efficiency of the compressor unit as $\eta = 1.0$. Here, the crimson line has the critical temperature at the outlet of the cooling unit, that is, it is the same projection than that in Figure 3. At high temperatures, the optimal COP of the system decreases, while at lower temperatures, COP increases considerably. Moreover, a discontinuous line is indicated to represent the collection of all the optimal values of the COP directly obtained from eq 8 at different temperatures and compression ratio values. From this line, an operational limit of the transcritical line can be inferred, which is highlighted at point (A). At this point, the optimal value occurs at COP = 3.420, when the temperature is 302.55 K and the compression

https://dx.doi.org/10.1021/acsomega.0c02681
ACS Omega 2020, 5, 19217−19226

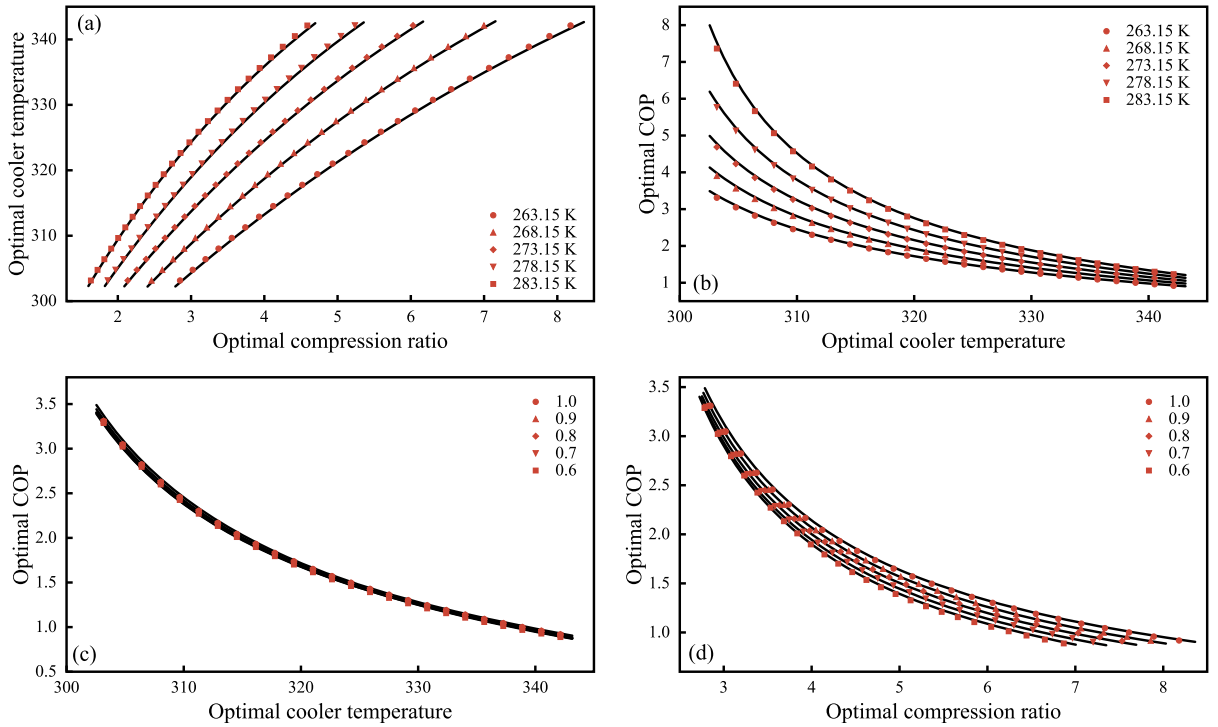

Figure 7. (a) Optimal value of the outlet temperature of the gas cooler as a function of the optimal compression ratio at different values of the temperature of the evaporator unit (T_1 = 263.15, 268.15, 273.15, 278.15, and 283.15 K) with an isentropic compressor, η = 1.0 (AAD 0.088%). (b) Optimal COP of the transcritical cycle as a function of the optimal compression ratio at different values of the evaporator temperature (T_1 = 263.15, 268.15, 273.15, 278.15, and 283.15 K) with an isentropic compressor, η = 1.0 (AAD 1.08%), (c) Optimal COP of the transcritical cycle as a function of the compression ratio at different efficiencies of the compressor unit (η = 0.6, 0.7, 0.8, 0.9, and 1.0) using an evaporator temperature of 263.16 K (AAD 0.81%), and (d) Optimal COP of the transcritical cycle as a function of temperature of the cooler at different efficiencies of the compressor unit (η = 0.6, 0.7, 0.8, 0.9, and 1.0) using an evaporator temperature of 263.16 K (AAD 0.81%). Continuous black lines are 17 while crimson symbols are Span–Wagner predictions.

is on the critical ratio. It is not possible to find an optimal value of the COP in transcritical operation below 302.55 K, although the COP will always be larger than the obtained at higher temperatures.

Now, the optimal point of operation of a transcritical cycle is unique if the temperature of the cooler is provided. Following this, Figure 5 shows a parametrical projection composed of all the optimal values of operation. Moreover, the optimum values are displayed at different efficiencies of the compression unit, taking values from η = 1.0 to 0.1, and the outlet of the cooling unit displayed from 302.55 K till 340.00 K. It is important to note that in Figure 5, the bolder black line represents the optimum at the isentropic operation of the compressor. Hence, this line renders the same limit shown in Figure 4. Moreover, some interesting remarks arise from Figure 5. First, the maximum COP is monotonically decreasing with the efficiency of the compression unit. The latter is seen in an example plotted in crimson dashed line at r = 4.0; from this point, the optimum COP is highlighted at point (A) when the compressor is isentropic, and while efficiency is decreasing (e.g. η = 0.2), the COP corresponds to point (B). It is important to note that each optimal value of COP is tied to a T_3 value. Therefore, point (A) and the continuous crimson line which arises from it lies at a temperature of 313.51 K, while point (B) lies at 322.68 K. Another intuitive observation is that over the black lines rendering the maximum COP at η = 1.0, there is not an optimal condition of operation. Regardless that, it is possible to find a higher COP if a lower temperature of the cooling unit is selected. From this diagram, a relationship between the efficiency of the compression process, the temperature of the outlet of the cooler, and the COP of the cycle is established.

2.3. Application of the Theoretically Based Control Function for CO_2 and N_2O. Remarkably, eq 8 is also a control function. This equation may be considered a general, theoretically based, and non-explicit control function. This is due to the fact that its mathematical formulation requires an internal model in order to obtain results. Interestingly, any control function and even graphical approaches can be developed from eq 8 under certain assumptions. Another advantage of the presented formulation is its model-free nature. Accordingly, this control function may be used for other working fluids of a transcritical cycle, as for example, nitrous oxide,[35,46] changing the model.

In order to illustrate the generality of eq 8, several well-established control functions are derived here. One of the most ingenious approaches for the optimization of a transcritical cycle was presented by Inokuty.[12,13] This methodology is a graphical approach, which can be obtained directly from eq 4. It is enough to consider an isentropic operation of the compressor, that is, η = 1.0 and hence $\partial\eta/\partial P_2 = 0$ and $\tilde{H}_2^r$ are merely $\tilde{H}_2$. Consequently, eq 4 yields

$$\left(\frac{d\tilde{H}_2}{dP_2}\right)_S \frac{\tilde{H}_1 - \tilde{H}_3}{\tilde{H}_2^r - \tilde{H}_1} + \left(\frac{d\tilde{H}_3}{dP_2}\right)_T = 0 \tag{11}$$

or

https://dx.doi.org/10.1021/acsomega.0c02681
ACS Omega 2020, 5, 19217−19226

$$\frac{1}{\tilde{H}_2^r - \tilde{H}_1}\left(\frac{d\tilde{H}_2}{dP_2}\right)_S = -\frac{1}{\tilde{H}_1 - \tilde{H}_3}\left(\frac{d\tilde{H}_3}{dP_2}\right)_T \quad (12)$$

Therefore, this intuitive and basic approach is reduced to the graphical calculation of the $\tilde{H}_2$ and $\tilde{H}_3$ derivatives as a function of P_2. This can be approximately performed using the pressure versus enthalpy diagram, as described in Figure 6. The optimum value of pressure will fulfil[12,13] the expression given by

$$\frac{\tilde{H}_2 - \tilde{H}_5}{\tilde{H}_2 - \tilde{H}_1} = -\frac{\tilde{H}_6 - \tilde{H}_3}{\tilde{H}_1 - \tilde{H}_3} \quad (13)$$

where $\tilde{H}_5$ and $\tilde{H}_7$ are two auxiliary points of enthalpy obtained from the $P-\tilde{H}$ graphic.

In a different contribution, Kauf[14] considered different ambient temperatures and concluded that the larger influence in COP comes from the aforementioned parameter. The same conclusion can be inferred by visual inspection of eq 8. The ambient temperature directly affects the extracted heat from the evaporator, while the energy required in the compressor is not sensitive to the outlet pressure, at least in the usual operation ranges. Moreover, Kauf considered that the temperature of the outlet of the cooler was 2.9 K higher than the ambient temperature. The application of eq 8 using this value, assuming an outlet evaporator temperature of 268.15 K (a datum not explicitly given in Kauf's contribution), and applying the multiparameter EOS for CO_2 with an isentropical operation for the compressor, provide the linear correlation proposed by this author, which is

$$P_2 = 2.59T_3 + 7.53 \quad (14)$$

Furthermore, the current control function presented in this contribution allows Kauf's function to be extended at different operating conditions of the evaporator unit. In this regard, it is enough to redefine the parameters of the control function as

$$P_2 = \theta_1 T_3 + \theta_2 \quad (15)$$

where θ_i are parameters depending on T_1, that is, the outlet temperature of the evaporator. Here, the parameters follow a linear form as

$$\theta_i = \theta_{i1} + \theta_{i2}T_1 \quad (16)$$

where the required parameters are listed in Table 1.

This extension qualitatively matches with another control function presented by Liao, Zhao, and Jakobsen[15] with $\eta = 1.0$. In fact, the control functions are useful tools because of their simplicity. Nevertheless, the origin of the control function limits its applicability when they are obtained by fitting to experimental or simulated data. Thus, the control functions are restricted mainly to the assumptions, the model, or data used in their construction and the range of these data used in the fitting. On the contrary, a model-free general control function, such as the one presented in eq 8, may be used to accurately develop tailor-made and adapted control functions for any range of conditions, models, or working fluids under controlled assumptions.

As an example, a new and accurate control function based on eq 8 is developed for CO_2 and N_2O. It is assumed that both the evaporator and the cooler are isobaric, the temperatures of the evaporator lies from 263.15 to 283.15 K, the outlet pressure of the compressor lies from the critical pressure of the working fluid to $r = 8$, and the efficiency of the compressor unit is assumed a fixed value, independent of the compression ratio. Besides, the cooler can reach temperatures from 302.55 K until 333.15 K for CO_2, while the temperature range of N_2O lies from from 308.00 K till 338.00 K. Moreover, the internal model is used as multi-parametric EOS for CO_2[4] and N_2O.[53] These kinds of EOS are accurate, and its utilization is often straightforward, being directly applicable to this developed function because of its mathematical structure formed by a function of the temperature and volume.

The volume after the isentropic compression may be fitted to empirical correlations,[54] which is obtained by linearizing the behavior of the properties as

$$\tilde{v}_2^r = \frac{\kappa_1}{\kappa_2 T_{3,r} + \kappa_3} \quad (17)$$

while the slope of the enthalpy at the point (3) is given by

$$\left(\frac{d\tilde{H}_3}{dP_2}\right)_T = \kappa_4 + \frac{\kappa_5}{\kappa_6 T_{3,r}^{\ 2} + \kappa_7 T_{3,r} + \kappa_8} \quad (18)$$

Additionally, the COP and the compression ratio are related as

$$\frac{COP}{\eta} = \kappa_9(\eta + \kappa_{10})\ln\left(\frac{\kappa_{11}\eta^{0.28}}{\eta + \kappa_{10}}r\right)^{-1} + \frac{\kappa_{12}}{\eta + \kappa_{10}} \quad (19)$$

where the parameters κ_i depend on the reduced temperature of the evaporator unit as polynomial as

$$\kappa_i = \kappa_{i,1}T_{1,r}^{\ 2} + \kappa_{i,2}T_{1,r} + \kappa_{i,3} \quad (20)$$

Table 2 summarizes the parameters for eq 20.

Furthermore, if the efficiency of the compression unit is not a fixed value, it is enough to have access to values of the heat of vaporization in the range of the correlation and to the vaporized fraction at the temperature of the evaporator. On the one hand, the heat of vaporization is widely available in correlations or can be fitted. Here, the heat of vaporization is obtained from

$$\Delta\tilde{H}_1 = \kappa_{13}(1 - T_{1,r})^{\kappa_{14}} \quad (21)$$

On the other hand, the vaporized fraction is given by

$$\Psi_1 = \kappa_{15}T_{3,r}^{\ 2} + \kappa_{16}T_{3,r} + \kappa_{17} \quad (22)$$

where the parameters κ_i are also given by eq 20.

The average absolute deviation (AADs) of the parametrisation proposed for the control function for both compounds are shown in Table 3.

The presented control function can accurately correlate the thermodynamic optimal variables of the transcritical cycle. As an example, the variables of the transcritical cycle with CO_2 as working fluid are shown in Figure 7a–c. These figures display simulated data obtained from the Span–Wagner EOS (symbols) compared with the results of the proposed control function (lines). Figure 7a shows the optimal cooler temperature as a function of the compression ratio of the cycle at different temperatures of the evaporator. In this figure, each point is associated to an optimal COP of the cycle. Furthermore, Figure 7b displays the optimal COP as a function of the optimal cooler temperature at different temperatures of the evaporator, while Figure 7c represents the variation of COP as the compression ratio changes and Figure 7d displays the optimal COP as a function of the

https://dx.doi.org/10.1021/acsomega.0c02681
ACS Omega 2020, 5, 19217−19226

optimal cooler temperature at different isentropic efficiencies. An excellent agreement is found between the Span−Wagner calculated data and the calculations of the control function. The parametrized control function can be used separately, for example, to obtain the COP from a given compression ratio via eq 19 or altogether, for example, to obtain the cooler temperature from the compression ratio and evaporator temperature via eqs 17−19. Table 3 summarizes the AADs of different calculations using the proposed control function.

Finally, it is important to remark that other control functions of similar origin may be obtained as a function of other desired variables using an adequate EOS, experimental, or simulation data for the desired fluid.

3. CONCLUDING REMARKS

This work has been devoted to developing a rigorous and accurate framework in order to predict and optimize the performance of transcritical cycles by means of tailor-made control functions using carbon dioxide (CO_2) and nitrous oxide (N_2O) as examples. This development is directly relevant to any equation of state depending on the Helmholtz variable group. The presented mathematical development constitutes a non-explicit general control function, and it may be coupled to any internal model to obtain results. For this reason, it is especially suitable for mathematically convoluted EOSs such as the SAFT-family of EOSs or multi-parametric EOSs. The results have shown that the optimal compressor ratio is not sensitive to the efficiency of the compressor, becoming independent on the COP, which −as expected− has substantial variations when the efficiency of the compression changes. Considering the presented approach and the Span−Wagner multi-parametric EOS, a new and accurate control function based on the presented mathematics is provided. The generalized expression can be reduced to other control functions found in the literature. In addition, this control function can model the critical variables of a transcritical cycle to obtain data or to optimize its variables. The versatility of the presented approach provides a tool able to be extended to other types of cycles and to other compounds or azeotropic mixtures using models depending on the Helmholtz variable group.

AUTHOR INFORMATION

Corresponding Authors

José Matías Garrido − *Departamento de Ingeniería Química, Faculty of Engineering, Universidad de Concepción, 4030000 Concepción, Chile;* orcid.org/0000-0001-9989-7206; Email: josemagarrido@udec.cl

Héctor Quinteros-Lama − *Departamento de Tecnologías Industriales, Faculty of Engineering, Universidad de Talca, 3340000 Curicó, Chile;* orcid.org/0000-0001-8953-6140; Email: hquinteros@me.com

Authors

Johan González − *Departamento de Tecnologías Industriales, Faculty of Engineering, Universidad de Talca, 3340000 Curicó, Chile;* orcid.org/0000-0001-8740-8743

Fèlix Llovell − *Department of Chemical Engineering and Materials Science, IQS School of Engineering, Universitat Ramon Llull, 08017 Barcelona, Spain;* orcid.org/0000-0001-7109-6810

Complete contact information is available at: https://pubs.acs.org/10.1021/acsomega.0c02681

Notes

The authors declare no competing financial interest.

ACKNOWLEDGMENTS

J. Gonzalez acknowledges doctoral scholarships from CONICYT, Chile (no. 21180578) and program Doctorado en Sistemas de Ingeniería of the Universidad de Talca, H.Q.-L. acknowledges funding from FONDECYT, Chile (project no. 11180103) and J.M.G. acknowledges funding from FONDECYT, Chile (project no. 11170111). Additional funding has been provided by project 2019-URL-IR1rQ-011, from Obra Social "La Caixa".

LIST OF SYMBOLS

Q:extracted heat at the evaporation unit.; W:work of the compression unit.; $\tilde{H}_i$:molar enthalpy at point i.; P_i:pressure at point i.; T_i:thermodynamic temperature at point i.; $\tilde{v}_i$:molar volume at point i.; $\tilde{S}_i$:molar entropy at point i.; $\tilde{G}_i$:Gibbs energy function at point i.; $\Delta\tilde{H}_i$:heat of vaporisation in the point i.; $\tilde{A}$:Helmholtz energy function.; r:compression ratio defined as P_2/P_1.; a_i, b_i, c_i, d_i and m_i:coefficients for the control functions.

SUBSCRIPTS AND SUPERSCRIPTS

op:refers to the optimal condition.; r:as superscript refers to an isentropic process and as subscript refers to a reduced property.

GREEK LETTERS

η: efficiency of the compression unit.; κ_i: coefficients of the empirical correlation for the efficiency of the compression unit.; Ψ_i: vaporised fraction at point i.

ABBREVIATIONS

EOS: equation of state; ODP: ozone depletion potential; GWP: global warming potential; CFC: chlorofluorocarbon; HCFC: hydrochlorofluorocarbon; HFC: hydrofluorocarbon; COP: coefficient of performance; SAFT: statistical association fluid theory

REFERENCES

(1) United nations environment Programme. *Montreal Protocol and Green Economy*; Markandya, A., Dale, N., Eds.; Assessing the contributions and co-benefits of a Multilateral Environmental Agreement, 2012.

(2) Elakdhar, M.; Nehdi, E.; Kairouani, L. Analysis of a Compression/Ejection Cycle for Domestic Refrigeration. *Ind. Eng. Chem. Res.* **2007**, *46*, 4639−4644.

(3) IISDs SDG Knowledge Hub. *Kigali Amendment Enters into Force, Bringing Promise of Reduced Global Warming|News|SDG Knowledge Hub|IISD*, retrieved March, 7 2019.

(4) Span, R.; Wagner, W. A new equation of state for carbon dioxide covering the fluid region from the triple-point temperature to 1100 K at pressures up to 800 MPa. *J. Phys. Chem. Ref. Data* **1996**, *25*, 1509−1596.

(5) Richter, M. R.; Song, S. M.; Yin, J. M.; Kim, M. H.; Bullard, C. W.; Hrnjak, P. S. Experimental results of transcritical CO_2 heat pump for residential application. *Energy* **2003**, *28*, 1005−1019.

(6) Manjili, F. E.; Cheraghi, M. Performance of a new two-stage transcritical CO2 refrigeration cycle with two ejectors. *Appl. Therm. Eng.* **2019**, *156*, 402−409.

(7) Yang, L.-X.; Wei, X.-L.; Zhao, L.-H.; Qin, X.; Zhang, D.-W. Experimental study on the effect of compressor frequency on the performance of transcritical CO2 heat pump system with regenerator. *Appl. Therm. Eng.* **2019**, *150*, 1216−1223.

(8) Song, Y.; Cui, C.; Li, M.; Cao, F. Investigation on the effects of the optimal medium-temperature on the system performance in a transcritical CO2 system with a dedicated transcritical CO2 subcooler. *Appl. Therm. Eng.* **2020**, *168*, 114846.
(9) Lorentzen, G.; Pettersen, J. A new, efficient and environmentally benign system for car air-conditioning. *Int. J. Refrig.* **1993**, *16*, 4−12.
(10) Ma, Y.; Liu, Z.; Tian, H. A review of transcritical carbon dioxide heat pump and refrigeration cycles. *Energy* **2013**, *55*, 156−172.
(11) Calm, J. M. The next generation of refrigerants − Historical review, considerations, and outlook. *Int. J. Refrig.* **2008**, *31*, 1123−1133.
(12) Inokuty, H. Approximate graphical method of finding compression pressure of CO_2refrigerant machine for maximum Coefficient of Performance. *92th Japan Society of Mechanical Engineers*, 1923.
(13) Inokuty, H. Zeichnerisches verfahren zum auffinden des günstigsten kondensatordruckes in kohlensäurekältemaschinen. *Z. Gesamte Strafr.* **1928**, *35*, 180−182.
(14) Kauf, F. Determination of the optimum high pressure for transcritical CO_2-refrigeration cycles. *Int. J. Therm. Sci.* **1999**, *38*, 325−330.
(15) Liao, S. M.; Zhao, T. S.; Jakobsen, A. A correlation of optimal heat rejection pressures in transcritical carbon dioxide cycles. *Appl. Therm. Eng.* **2000**, *20*, 831−841.
(16) Sarkar, J.; Bhattacharyya, S.; Gopal, M. R. Optimization of a transcritical CO_2 heat pump cycle for simultaneous cooling and heating applications. *Int. J. Refrig.* **2004**, *27*, 830−838.
(17) Chen, Y.; Gu, J. The optimum high pressure for CO_2 transcritical refrigeration systems with internal heat exchangers. *Int. J. Refrig.* **2005**, *28*, 1238−1249.
(18) Sawalha, S. Theoretical evaluation of trans-critical CO_2 systems in supermarket refrigeration. Part I: Modeling, simulation and optimization of two system solutions. *Int. J. Refrig.* **2008**, *31*, 516−524.
(19) Kim, S. C.; Won, J. P.; Kim, M. S. Effects of operating parameters on the performance of a CO_2 air conditioning system for vehicles. *Appl. Therm. Eng.* **2009**, *29*, 2408−2416.
(20) Aprea, C.; Maiorino, A. Heat rejection pressure optimization for a carbon dioxide split system: An experimental study. *Appl. Energy* **2009**, *86*, 2373−2380.
(21) Ge, Y. T.; Tassou, S. A. Performance evaluation and optimal design of supermarket refrigeration systems with supermarket model "SuperSim". Part II: Model applications. *Int. J. Refrig.* **2011**, *34*, 540−549.
(22) Zhang, X. P.; Wang, F.; Fan, X. W.; Wei, X. L.; Wang, F. K. Determination of the optimum heat rejection pressure in transcritical cycles working with R744/R290 mixture. *Appl. Therm. Eng.* **2013**, *54*, 176−184.
(23) Qi, P.-C.; He, Y.-L.; Wang, X.-L.; Meng, X.-Z. Experimental investigation of the optimal heat rejection pressure for a transcritical CO_2 heat pump water heater. *Appl. Therm. Eng.* **2013**, *56*, 120−125.
(24) Yang, L.; Li, H.; Cai, S.-W.; Shao, L.-L.; Zhang, C.-L. Minimizing COP loss from optimal high pressure correlation for transcritical CO_2 cycle. *Appl. Therm. Eng.* **2015**, *89*, 656−662.
(25) Sarkar, J.; Bhattacharyya, S.; Gopal, M. R. Simulation of a transcritical CO_2 heat pump cycle for simultaneous cooling and heating applications. *Int. J. Refrig.* **2006**, *29*, 735−743.
(26) Yari, M. Performance analysis and optimization of a new two-stage ejector-expansion transcritical CO_2 refrigeration cycle. *Int. J. Therm. Sci.* **2009**, *48*, 1997−2005.
(27) Sarkar, J. Optimization of ejector-expansion transcritical CO_2 heat pump cycle. *Energy* **2008**, *33*, 1399−1406.
(28) Bhattacharyya, S.; Mukhopadhyay, S.; Kumar, A.; Khurana, R. K.; Sarkar, J. Optimization of a CO_2−C_3H_8 cascade system for refrigeration and heating. *Int. J. Refrig.* **2005**, *28*, 1284−1292.
(29) Cecchinato, L.; Corradi, M.; Cosi, G.; Minetto, S.; Rampazzo, M. A real-time algorithm for the determination of R744 systems optimal high pressure. *Int. J. Refrig.* **2012**, *35*, 817−826.
(30) Zhang, W.-J.; Zhang, C.-L. A correlation-free on-line optimal control method of heat rejection pressures in CO_2 transcritical systems. *Int. J. Refrig.* **2011**, *34*, 844−850.
(31) Cecchinato, L.; Corradi, M.; Minetto, S. A critical approach to the determination of optimal heat rejection pressure in transcritical systems. *Appl. Therm. Eng.* **2010**, *30*, 1812−1823.
(32) Minetto, S. Theoretical and experimental analysis of a CO_2 heat pump for domestic hot water. *Int. J. Refrig.* **2011**, *34*, 742−751.
(33) Cabello, R.; Sánchez, D.; Llopis, R.; Torrella, E. Experimental evaluation of the energy efficiency of a CO_2 refrigerating plant working in transcritical conditions. *Appl. Therm. Eng.* **2008**, *28*, 1596−1604.
(34) Shao, L.-L.; Zhang, Z.-Y.; Zhang, C.-L. Constrained optimal high pressure equation of CO2 transcritical cycle. *Appl. Therm. Eng.* **2018**, *128*, 173−178.
(35) Zhang, Z.; Hou, Y.; Kulacki, F. A. Theoretical analysis of a transcritical double-stage nitrous oxide refrigeration cycle with an internal heat exchanger. *Appl. Therm. Eng.* **2018**, *140*, 147−157.
(36) Wu, C.; Wang, S.-s.; Jiang, X.; Li, J. Thermodynamic analysis and performance optimization of transcritical power cycles using CO_2-based binary zeotropic mixtures as working fluids for geothermal power plants. *Appl. Therm. Eng.* **2016**, *115*, 1−64.
(37) Xia, J.; Wang, J.; Zhang, G.; Lou, J.; Zhao, P.; Dai, Y. Thermo-economic analysis and comparative study of transcritical power cycles using CO2-based mixtures as working fluids. *Appl. Therm. Eng.* **2018**, *144*, 31−44.
(38) Smith, J. M.; van Ness, H. C.; Abbott, M. M. *Introduction to Chemical Engineering Thermodynamics*; McGraw-Hill: New York, 2005.
(39) Bai, T.; Yan, G.; Yu, J. Thermodynamics analysis of a modified dual-evaporator CO_2 transcritical refrigeration cycle with two-stage ejector. *Energy* **2015**, *84*, 1−11.
(40) Baheta, A. T.; Hassan, S.; Reduan, A. R. B.; Woldeyohannes, A. D. Performance investigation of transcritical carbon dioxide refrigeration cycle. *Procedia CIRP* **2015**, *26*, 482−485.
(41) Jamali, S.; Yari, M.; Mohammadkhani, F. Performance improvement of a transcritical CO_2 refrigeration cycle using two-stage thermoelectric modules in sub-cooler and gas cooler. *Int. J. Refrig.* **2016**, *74*, 105−115.
(42) Rawat, K. S.; Bisht, V. S.; Pratihar, A. K. Thermodynamic analysis and optimization of CO_2 based transcritical cycle. *iJRASET* **2015**, *3*, 287−293.
(43) Beegle, B. L.; Modell, M.; Reid, R. C. Legendre transforms and their application in thermodynamics. *AIChE J.* **2004**, *20*, 1194−1200.
(44) Brodal, E.; Jackson, S. A comparative study of CO_2 heat pump performance for combined space and hot water heating. *Int. J. Refrig.* **2019**, *108*, 234−245.
(45) Chen, G.; Volovyk, O.; Zhu, D.; Ierin, V.; Shestopalov, K. Theoretical analysis and optimization of a hybrid SO_2 transcritical mechanical compression − ejector cooling cycle. *Int. J. Refrig.* **2016**, *74*, 1−29.
(46) Dokandari, D. A.; Mahmoudi, S. M. S.; Bidi, M.; Khoshkhoo, R. H.; Rosen, M. A. First and Second Law Analyses of Trans-critical N2O Refrigeration Cycle Using an Ejector. *Sustainability* **2018**, *10*, 1177−1214.
(47) Rowlinson, J. S. *Liquids & Liquid Mixtures*, 3rd ed.; Butterworths Scientific: London, 1982.
(48) Span, R. *Multiparameter Equations of State: an Accurate Source of Thermodynamic Property Data*; Springer Verlag: Berlin, Heidelberg, 2000.
(49) Fang, Y.; De Lorenzo, M.; Lafon, P.; Poncet, S.; Bartosiewicz, Y. An accurate and efficient look-up table equation of state for two-phase compressible flow simulations of carbon dioxide. *Ind. Eng. Chem. Res.* **2018**, *57*, 7676−7691.
(50) Chapman, W. G.; Gubbins, K. E.; Jackson, G.; Radosz, M. SAFT: equation-of-state solution model for associating fluids. *Fluid Phase Equilib.* **1989**, *52*, 31−38.

https://dx.doi.org/10.1021/acsomega.0c02681
ACS Omega 2020, 5, 19217−19226

(51) Huang, S. H.; Radosz, M. Equation of state for small, large, polydisperse, and associating molecules. *Ind. Eng. Chem. Res.* **1990**, *29*, 2284−2294.
(52) Gross, J.; Sadowski, G. Perturbed-Chain SAFT: An equation of state based on a perturbation theory for chain molecules. *Ind. Eng. Chem. Res.* **2001**, *40*, 1244−1260.
(53) Lemmon, E. W.; Span, R. Short Fundamental Equations of State for 20 Industrial Fluids. *J. Chem. Eng. Data* **2006**, *51*, 785−850.
(54) Heidaryan, E. A. Note on Model Selection Based on the Percentage of Accuracy-Precision. *J. Energy Resour. Technol.* **2018**, *141*, 101201−101204.

https://dx.doi.org/10.1021/acsomega.0c02681
ACS Omega 2020, 5, 19217−19226